

Evidence for Single-gap Superconductivity in Mg(B<sub>1-x</sub>C<sub>x</sub>)<sub>2</sub> Single Crystals with x=0.132 from Point-Contact Spectroscopy

*Original*

Evidence for Single-gap Superconductivity in Mg(B<sub>1-x</sub>C<sub>x</sub>)<sub>2</sub> Single Crystals with x=0.132 from Point-Contact Spectroscopy / Gonnelli, Renato; Daghero, Dario; Calzolari, Andrea; Ummarino, Giovanni; Dellarocca, Valeria; Stepanov, V. A.; Kazakov, S. M.; Zhigadlo, N.; Karpinski, J.. - In: PHYSICAL REVIEW. B, CONDENSED MATTER AND MATERIALS PHYSICS. - ISSN 1098-0121. - STAMPA. - 71:6(2005), pp. 060503(R)-1-060503(R)-4. [10.1103/PhysRevB.71.060503]

*Availability:*

This version is available at: 11583/1400923 since:

*Publisher:*

APS American Physical Society

*Published*

DOI:10.1103/PhysRevB.71.060503

*Terms of use:*

This article is made available under terms and conditions as specified in the corresponding bibliographic description in the repository

*Publisher copyright*

(Article begins on next page)

## Evidence for single-gap superconductivity in $\text{Mg}(\text{B}_{1-x}\text{C}_x)_2$ single crystals with $x=0.132$ from point-contact spectroscopy

R. S. Gonnelli,<sup>1,2</sup> D. Daghero,<sup>1,2</sup> A. Calzolari,<sup>1</sup> G. A. Ummarino,<sup>1,2</sup> Valeria Dellarocca,<sup>1</sup> V. A. Stepanov,<sup>3</sup> S. M. Kazakov,<sup>4</sup> N. Zhigadlo,<sup>4</sup> and J. Karpinski<sup>4</sup>

<sup>1</sup>*Dipartimento di Fisica and INFM, Politecnico di Torino, 10129 Torino, Italy*

<sup>2</sup>*INFM - LAMIA, Corso Perrone 24, 16152 Genova, Italy*

<sup>3</sup>*P.N. Lebedev Physical Institute, Russian Academy of Sciences, 119991 Moscow, Russia*

<sup>4</sup>*Solid State Physics Laboratory, ETH, CH-8093 Zurich, Switzerland*

(Received 10 July 2004; revised manuscript received 3 December 2004; published 14 February 2005)

We report the results of the first directional point-contact measurements in  $\text{Mg}(\text{B}_{1-x}\text{C}_x)_2$  single crystals with  $0.047 \leq x \leq 0.132$ . The two-gap superconductivity typical of  $\text{MgB}_2$  persists up to  $x=0.105$ . In this region, the values of the gaps  $\Delta_\sigma$  and  $\Delta_\pi$  were determined by fitting the Andreev-reflection conductance curves with a two-band Blonder-Tinkham-Klapwijk (BTK) model, and confirmed by the single-band BTK fit of the  $\sigma$ - and  $\pi$ -band conductances, separated by means of a magnetic field. At  $x=0.132$ , when  $T_c=19$  K, we clearly observed the merging of the two gaps into one of amplitude  $\Delta \approx 3$  meV.

DOI: 10.1103/PhysRevB.71.060503

PACS number(s): 74.50.+r, 74.45.+c, 74.70.Ad

In the last three years, the great experimental and theoretical efforts of the scientific community have led to a clarification of most features of the intermetallic superconductor  $\text{MgB}_2$ . These features are mainly related to the presence of two band systems ( $\sigma$  and  $\pi$ ) and of the relevant gaps.<sup>1,2</sup> Point-contact spectroscopy (PCS) has proved particularly useful in measuring both the  $\sigma$ - and  $\pi$ -band gaps at the same time<sup>3,4</sup> and determining the temperature dependency of these gaps with great accuracy.<sup>4</sup> Very soon after the discovery of superconductivity in  $\text{MgB}_2$ , substitutions of Al for Mg and of C for B were tried, in order to introduce impurities in the compound and modify its superconducting properties.<sup>5</sup> In particular, nearly single-phase  $\text{Mg}(\text{B}_{1-x}\text{C}_x)_2$  polycrystals with  $0.09 \leq x \leq 0.13$  were obtained by starting from Mg and  $\text{B}_4\text{C}$ ,<sup>6,7</sup> which showed a linear dependence of the cell parameter  $a$  on the C concentration.<sup>7</sup> More recently, C-substituted  $\text{MgB}_2$  single crystals were grown and many of their structural, superconducting and transport properties were measured.<sup>8,9</sup> The first STM and PCS measurements on polycrystalline  $\text{Mg}(\text{B}_{1-x}\text{C}_x)_2$  have shown the persistence of the two gaps up to  $x=0.1$ .<sup>10-12</sup> Up to now, the predicted achievement of single-gap superconductivity at a very high impurity level has never been observed.

This paper presents the results of PCS measurements in  $\text{Mg}(\text{B}_{1-x}\text{C}_x)_2$  single crystals with  $0.047 \leq x \leq 0.132$ , in the presence of magnetic fields up to 9 T either parallel or perpendicular to the  $c$  axis. These measurements gave us the dependence of the two gaps ( $\Delta_\pi$  and  $\Delta_\sigma$ ) on the carbon content  $x$  and showed that, up to  $x \approx 0.10$ , the two-gap superconductivity typical of unsubstituted  $\text{MgB}_2$  is retained. At  $x=0.132$ , we clearly and reproducibly observed the merging of  $\Delta_\pi$  and  $\Delta_\sigma$  into a single gap  $\Delta=3.2 \pm 0.9$  meV, which gives a ratio  $2\Delta/k_B T_c$  very close to the standard BCS value.

The high-quality  $\text{Mg}(\text{B}_{1-x}\text{C}_x)_2$  single crystals were grown at ETH (Zurich) with the same high-pressure technique adopted for unsubstituted  $\text{MgB}_2$ ,<sup>9</sup> and by using either graphite powder or silicon carbide as a carbon source. Details on the structural and superconducting properties of these crys-

tals can be found in a recent paper.<sup>9</sup> The seven different carbon contents of our crystals were estimated from the lattice parameter  $a$ , by assuming its linear dependence on  $x$ .<sup>7</sup> The resulting  $x$  values range between  $x=0.047$  and  $x=0.132$ , corresponding to bulk critical temperatures between 35 and 19 K.

We performed PCS measurements with the current mainly injected along the  $ab$  planes of the crystal, since in unsubstituted  $\text{MgB}_2$  this is the most favorable configuration for the contemporaneous measurement of both gaps.<sup>2,4</sup> The point contacts were thus made on the flat side surface of the crystals (not thicker than 80  $\mu\text{m}$ ) by using a small ( $\varnothing \approx 50$   $\mu\text{m}$ ) spot of Ag conductive paint. This "soft" version of the PCS technique<sup>4,13</sup> yields greater contact stability on thermal cycling and greater reproducibility of the conductance curves. By applying short current or voltage pulses to the junctions, we were able to tune their characteristics and achieve in most cases a normal-state resistance between 50 and 300  $\Omega$ . Since the in-plane mean free path in these single crystals ranges from  $\ell \approx 17.5$  nm to  $\ell \approx 13$  nm for  $x$  between 0.05 and 0.095,<sup>9</sup> these junctions result in the ballistic regime. The formation of parallel microjunctions explains the very few cases in which ballistic conduction is observed in low-resistance contacts.

Figure 1 reports some experimental conductance curves ( $dI/dV$  vs  $V$ ) of point contacts on crystals with different C contents (symbols). The curves are normalized as explained in Ref. 4. As already shown by PCS in  $\text{Mg}(\text{B}_{1-x}\text{C}_x)_2$  polycrystals,<sup>12</sup> when  $x \geq 0.047$  the experimental curves do not show the clear four-peak structure typical of  $ab$ -plane contacts on unsubstituted  $\text{MgB}_2$ .<sup>4</sup> Hence, the proof of the presence of the  $\sigma$ -band gap and its determination require a fit with the two-band BTK model<sup>3,4,11-13</sup> and/or the selective suppression of the  $\pi$ -band contribution to the conductance, e.g., by applying a suitable magnetic field.<sup>4,13</sup> In the following we will present and discuss both these approaches.

First, let us discuss the fit of the zero-field conductance curves reported in Fig. 1. In the two-band BTK model the

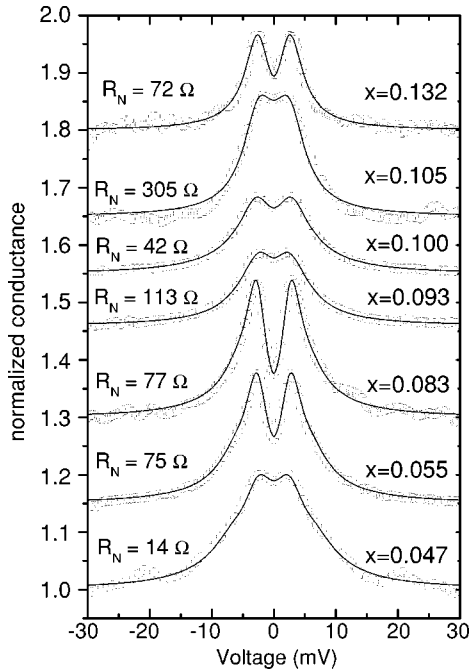


FIG. 1. Normalized conductance curves at 4.2 K of different *ab*-plane junctions in  $\text{Mg}(\text{B}_{1-x}\text{C}_x)_2$  crystals with  $0.047 \leq x \leq 0.132$  (open circles) and their two- or single-band BTK fits (solid lines). The curves are vertically shifted for clarity. The best-fitting values of the parameters are shown in Table I.

normalized conductance of a point contact is given by  $\sigma = (1 - w_\pi)\sigma_\sigma + w_\pi\sigma_\pi$  where  $\sigma_\sigma$  and  $\sigma_\pi$  are the partial  $\sigma$ - and  $\pi$ -band conductances, respectively, and  $w_\pi$  is the weight of the  $\pi$ -band contribution. Thus, the total number of parameters in the model is 7. In unsubstituted  $\text{MgB}_2$ ,  $w_\pi$  ranges from 0.66 to 0.99, as theoretically predicted<sup>2</sup> and confirmed by directional PCS.<sup>4</sup> In the absence of a similar prediction for the C-substituted compound, we conservatively took  $w_\pi$  between 0.66 and 0.8.

For any  $x$  between 0.047 and 0.105, the two-band BTK model fits very well the experimental data, as shown in Fig. 1 (solid lines). The best-fitting parameters are listed in Table I. In the crystals with the highest C content, i.e.,  $x=0.132$ , the two-band BTK fit requires gap values very close to each other and, practically, interchangeable (in the sense that their error bars largely overlap). Actually, a fit with the standard

TABLE I. Values of the gaps and of the broadening parameters for the best-fit curves of Fig. 1 (solid lines).  $Z_\sigma$  is always close to 0.50 and  $Z_\pi$  ranges between 0.34 and 0.57. Note that the values of  $\Delta$  and  $\Gamma$  at  $x=0.132$  are reported in the  $\sigma$ -band cells only for convenience.

$x$	0.047	0.055	0.083	0.093	0.100	0.105	0.132
$\Delta_\sigma$	7.0	6.6	5.8	4.3	4.9	4.25	2.8
$\Delta_\pi$	3.2	3.0	3.0	2.8	3.3	3.2	–
$\Gamma_\sigma$	3.15	2.50	2.60	3.20	4.55	2.55	1.50
$\Gamma_\pi$	1.60	1.10	0.91	2.00	2.07	1.62	–
$w_\pi$	0.66	0.75	0.70	0.70	0.69	0.80	0

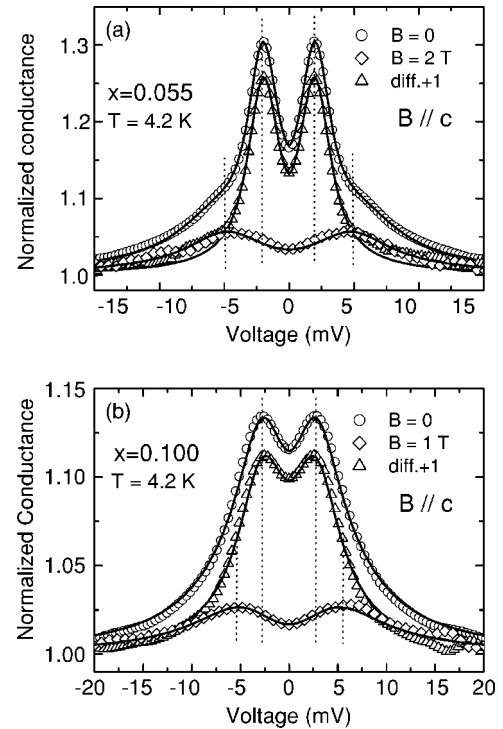


FIG. 2. (a) Normalized conductance curves of an *ab*-plane contact in a crystal with  $x=0.055$ , at  $B=0$  (circles) and  $B=2$  T (diamonds). Triangles represent the difference of the previous two curves, shifted by 1. Solid lines: best-fitting curves given by the two-band (upper curve) or single-band (lower curves) BTK model: (b) same as in (a), but for a crystal with  $x=0.100$ . Here the applied magnetic field is  $B=1$  T. Vertical lines indicate the conductance peaks.

*single-band* BTK model works even better. The solid line superimposed to the conductance curve at  $x=0.132$  in Fig. 1 is indeed obtained with only one gap of amplitude  $\Delta = 2.8 \pm 0.2$  meV.

The reliability of the determination of  $\Delta_\sigma$  and  $\Delta_\pi$  by means of a seven-parameter fit may be questioned. We thus tried to apply here the procedure we already used in unsubstituted  $\text{MgB}_2$ ,<sup>4</sup> that consists in separating the partial  $\sigma$ - and  $\pi$ -band contributions to the total conductance ( $\sigma_\sigma$  and  $\sigma_\pi$ ) by means of a suitable magnetic field, and in fitting each of them with the standard, three-parameter BTK model. A detailed discussion of the applicability of the BTK fit of Andreev-reflection curves in the presence of magnetic fields is given in Ref. 13.

Figure 2 shows how this works in crystals with (a)  $x=0.055$  and (b)  $x=0.100$ . In both panels, the zero-field conductance  $\sigma_0$  (circles) is compared to the relevant two-band BTK fit (solid line). Diamonds represent instead the conductance  $\sigma_{B^*}$  measured in a magnetic field  $B^*$  (making an angle  $\varphi = 90^\circ \pm 2^\circ$  with the *ab* planes) that completely removes any structure related to the  $\pi$ -band gap.<sup>21</sup> For  $x=0.055$ ,  $B^* \approx 2$  T, while for  $x=0.100$   $B^*=1$  T, as in unsubstituted  $\text{MgB}_2$ . Incidentally, this indicates that  $B^*$  has a maximum somewhere between  $x=0$  and  $x=0.100$ , like the critical field<sup>14,15</sup> and the irreversibility field.<sup>16</sup>  $\sigma_{B^*}$  contains only the  $\sigma$ -band contribution to the conductance and can thus be fitted

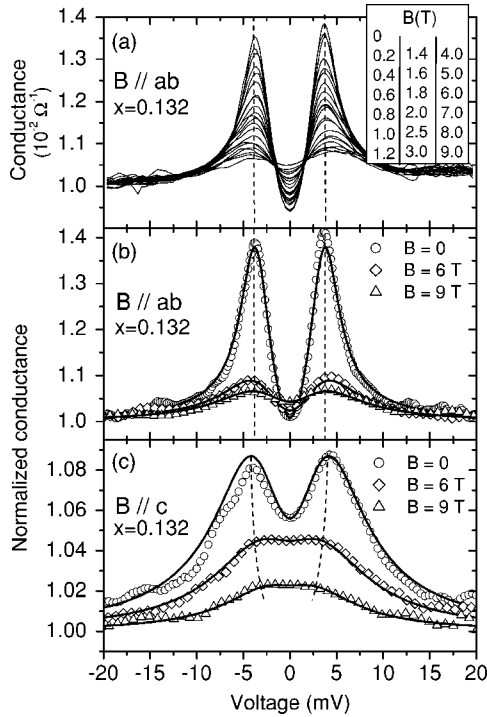


FIG. 3. (a) Raw conductance curves at  $T=4.2$  K in a crystal with  $x=0.132$ , in a magnetic field  $\mathbf{B}\parallel ab$ ; (b) some of these curves after normalization (symbols). Solid lines are the single-band BTK fits. On increasing the field from 0 to 9 T, the best-fit parameters vary as follows:  $\Delta=4.0\text{--}3.5$  meV,  $\Gamma=0.8\text{--}3.8$  meV,  $Z=0.60\text{--}0.53$ ; (c) same as in (b), but with  $\mathbf{B}\parallel c$ . Here, the parameters vary as follows:  $\Delta=4.0\text{--}2.0$  meV,  $\Gamma=3.6\text{--}4.6$  meV,  $Z=0.52\text{--}0.42$ . In (a), (b), and (c), dashed lines indicate the conductance peaks.

by taking  $\sigma_\pi=1$  in the two-band BTK model. Since  $w_\pi$  is reasonably field independent, only  $\Delta_\sigma$ ,  $\Gamma_\sigma$  and  $Z_\sigma$  remain as adjustable parameters. Finally, the difference  $\sigma_{\text{diff}}=\sigma_0-\sigma_{B^*}+1$  (triangles) contains only the  $\pi$ -band conductance and can thus be fitted by taking  $\sigma_\sigma=1$  in the two-band BTK model.<sup>4</sup>

The separate fit of  $\sigma_\sigma$  and  $\sigma_\pi$  gives the following results: (a)  $\Delta_\sigma=5.45$  meV,  $Z_\sigma=0.475$ ,  $\Gamma_\sigma=2.4$  meV and  $\Delta_\pi=2.30$  meV,  $Z_\pi=0.488$ ,  $\Gamma_\pi=0.485$  meV; (b)  $\Delta_\sigma=4.9$  meV,  $Z_\sigma=0.525$ ,  $\Gamma_\sigma=4.55$  meV and  $\Delta_\pi=3.28$  meV,  $Z_\pi=0.42$ ,  $\Gamma_\pi=2.07$  meV. In the case of  $x=0.055$ , a slight reduction in  $\Delta_\sigma$  (smaller than the gap distribution width, see Fig. 5) is present with respect to the two-band fit (that gave  $\Delta_\sigma=6.05$  meV and  $\Delta_\pi=2.35$  meV), possibly because  $B^*=2$  T is already comparable to  $B_{c2}^{\parallel c}\simeq 8$  T.<sup>9</sup> For the case of  $x=0.100$ , the parameters coincide with those reported in Table I. Similar agreement was found for any C content up to  $x=0.105$ , and in all the junctions we studied, showing that this procedure has a high level of internal consistency and gives precise and reliable results, as in unsubstituted  $\text{MgB}_2$ .<sup>4</sup>

In the crystals with  $x=0.132$ , the same procedure gives quite different results and further confirms the presence of a single gap. Figure 3(a) reports an example of magnetic-field dependence of the raw conductance curves, for  $\mathbf{B}\parallel ab$ . Contrary to what happens at lower C contents, there is no clear shift of the conductance maxima towards higher energy (which is the hallmark of the suppression of the  $\pi$ -band con-

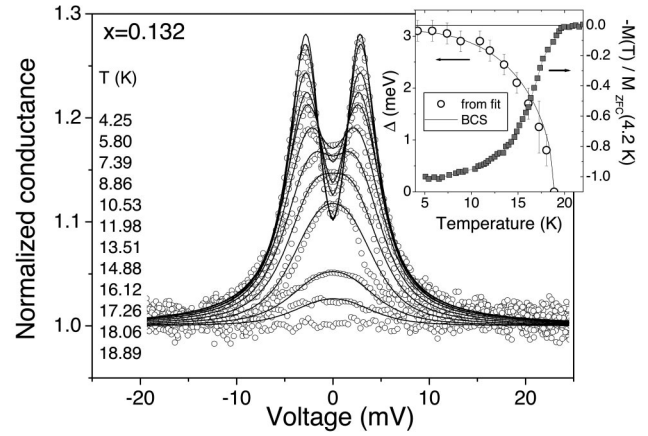


FIG. 4. Example of temperature dependence of the normalized conductance curves for  $x=0.132$  (symbols) with the relevant fit (solid lines). The gap given by the fit (inset, open symbols) follows very well the BCS  $\Delta(T)$  curve (inset, line). Filled symbols in the inset represent the ZFC magnetization.

tribution at  $B=B^*$ ) at any field between 0 and 9 T. Rather, the peaks approximately remain in the same position, as indicated by vertical dashed lines. In Fig. 3(b) the curves at  $B=0$  (circles),  $B=6$  T (diamonds), and  $B=9$  T (triangles) are shown after normalization. Similarly, Fig. 3(c) reports the normalized conductance curves of another contact, measured at the same fields but in the  $\mathbf{B}\parallel c$  configuration. In both (b) and (c), the experimental curves are compared to their single-band BTK fit, whose parameters are reported in the caption. The good quality of the fit and the magnetic-field dependence of the conductance curves strongly indicate that, at  $x=0.132$ ,  $\text{Mg}(\text{B}_{1-x}\text{C}_x)_2$  is an anisotropic single-gap superconductor with  $B_{c2}^{\parallel ab} > B_{c2}^{\parallel c} > 9$  T.

Further support to the presence of a single gap in crystals with  $x=0.132$  comes from the temperature dependence of the conductance curves, shown in the main panel of Fig. 4. All the experimental curves (symbols) can be fitted by the single-band BTK model (solid lines), and the resulting gap values (inset, open circles) follow very well the BCS curve with  $2\Delta/k_B T_c=3.8$  (inset, line). A comparison of  $\Delta(T)$  with the ZFC magnetization (inset, filled squares) shows that the critical temperature of the junction coincides with the bulk  $T_c$  and that the magnetic transition is complete at 5 K.

The dependence of the gaps on the carbon content and on the bulk  $T_c$  is reported in Figs. 5(a) and 5(b), respectively. Each point results from an average of various gap values (usually 4–8) obtained in different contacts. Hence, error bars indicate the maximum spread of measured values, and give an idea of the good reproducibility of our results. The value of the single gap at  $x=0.132$ ,  $\Delta=3.2\pm 0.9$  meV, and the bulk  $T_c=19$  K give a gap ratio  $2\Delta/k_B T_c\sim 3.9$  close to the BCS value. Despite the large uncertainty on  $\Delta$ , all the curves at  $x=0.132$  were best-fitted by a single gap BTK model. Note that the gap merging at  $x=0.132$  is perfectly consistent with the regular and smooth trend of the gaps for lower C contents. The decrease in  $\Delta_\sigma$  and the slight increase in  $\Delta_\pi$  shown in Fig. 5 suggest an increase in interband scattering, as predicted by the two-band model.<sup>1</sup> However, interband

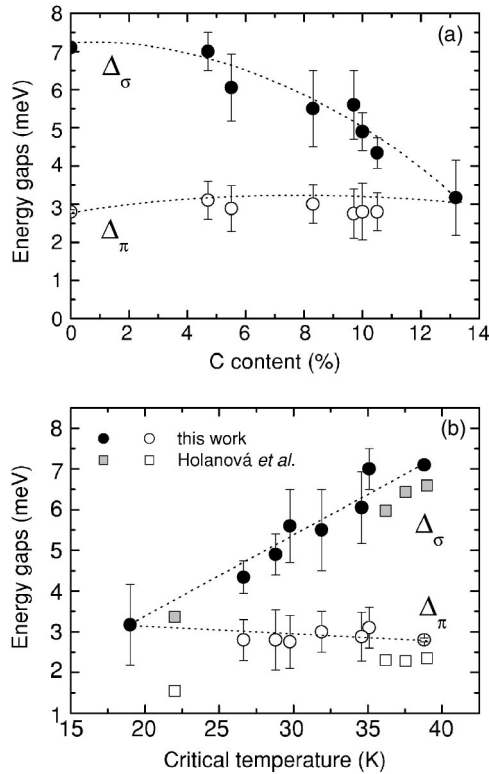


FIG. 5. Gap amplitudes,  $\Delta_\sigma$  and  $\Delta_\pi$ , as a function of the C content  $x$  (a) and of the bulk critical temperature  $T_c$  (b). In the latter case, data from PCS in polycrystals (Ref. 12) are reported for comparison. Dotted lines are guides to the eye.

scattering alone would make the gaps merge in a isotropic gap  $\Delta \approx 4$  meV when  $T_c = 26$  K. Clearly, other effects are playing a role, such as the changes in the electronic structure due to electron doping<sup>17</sup> and the hardening and narrowing of the  $E_{2g}$  phonon mode.<sup>14</sup> By taking into account these effects, the observed  $\Delta_\sigma(x)$  and  $\Delta_\pi(x)$  curves in  $\text{Mg}(\text{B}_{1-x}\text{C}_x)_2$  single crystals (included their merging at  $T_c = 19$  K) can be well explained within the two-band Eliashberg theory as resulting from the band filling, plus a decrease in the Coulomb pseudopotential and an *increase* in interband scattering<sup>18,19</sup>

even though this contrasts with the theoretical prediction that C substitution should have negligible effects on the  $\sigma$ - $\pi$  scattering.<sup>20</sup>

In Fig. 5(b), our gap values are compared to data from PCS in polycrystals by Holánová *et al.*<sup>12</sup> Apart from a small systematic shift, their  $\Delta_\sigma(T)$  curve is in good agreement with our results in the whole doping range, while their value of  $\Delta_\pi$  at  $x=0.10$  ( $T_c=22$  K), is much smaller than ours. This disagreement is probably related to the greater amount of interband scattering in our crystals, which might be due to microscopic defects (also acting as pinning centers<sup>9</sup>) or to the existence of microdomains with ordered C distribution.<sup>19</sup> Both these possibilities are compatible with the presence of local C-content inhomogeneities on a scale comparable to  $\xi$ .<sup>9</sup> Finally, notice that the evidence of single-gap superconductivity at  $x=0.132$ , accompanied by an anisotropic band structure (see Fig. 3) is consistent with the extrapolation at  $x > 0.10$  of recent measurements of  $B_{c2}$  and Hall effect in single crystals up to  $x=0.10$ .<sup>14</sup>

In conclusion, we have presented the results of the first directional point-contact measurements in  $\text{Mg}(\text{B}_{1-x}\text{C}_x)_2$  single crystals with  $0.047 \leq x \leq 0.132$ , that allowed us to obtain the dependence of  $\Delta_\sigma$  and  $\Delta_\pi$  on the carbon content  $x$ . This dependence was confirmed by applying to the junctions a suitable magnetic field  $B^*$  able to remove the contribution of the  $\pi$ -band gap to the total conductance, thus allowing the separate determination of the gaps via a single-band BTK fit. Up to  $x \sim 0.10$ , the two-gap nature of superconductivity characteristic of unsubstituted  $\text{MgB}_2$  is retained. At  $x=0.132$  we clearly and reproducibly observed the merging of the two gaps into a single gap  $\Delta \approx 3$  meV with a gap ratio  $2\Delta/k_B T_c$  close to the standard BCS value and a critical field greater than 9 T.

This work was done within the INFM Project PRA “UMBRA,” the INTAS Project No. 01-0617 and the FIRB Project No. RBAU01FZ2P. V.A.S. acknowledges the support of RFBR Projects Nos. 04-02-17286 and 02-02-17133, and of the Russian Ministry of Science and Technology (Contract No. 40.012.1.1.1357). The work in Zurich was supported by the Swiss National Science Foundation, the NCCR Program MaNEP and ETH.

<sup>1</sup>A. Y. Liu *et al.*, Phys. Rev. Lett. **87**, 087005 (2001).

<sup>2</sup>A. Brinkman *et al.*, Phys. Rev. B **65**, 180517(R) (2001).

<sup>3</sup>P. Szabó *et al.*, Phys. Rev. Lett. **87**, 137005 (2001).

<sup>4</sup>R. S. Gonnelli *et al.*, Phys. Rev. Lett. **89**, 247004 (2002).

<sup>5</sup>R. J. Cava *et al.*, Physica C **385**, 8 (2003).

<sup>6</sup>R. A. Ribeiro *et al.*, Physica C **384**, 227 (2003).

<sup>7</sup>M. Avdeev *et al.*, Physica C **387**, 301 (2003).

<sup>8</sup>S. Lee *et al.*, Physica C **397**, 7 (2003).

<sup>9</sup>S. M. Kazakov *et al.*, Phys. Rev. B **71**, 024533 (2005).

<sup>10</sup>H. Schmidt *et al.*, Phys. Rev. B **68**, 060508(R) (2003).

<sup>11</sup>P. Samuely *et al.*, Phys. Rev. B **68**, 020505(R) (2003).

<sup>12</sup>Z. Holánová *et al.*, Phys. Rev. B **70**, 064520 (2004).

<sup>13</sup>R. S. Gonnelli *et al.*, Phys. Rev. B **69**, 100504(R) (2004).

<sup>14</sup>T. Masui *et al.*, Phys. Rev. B **70**, 024504 (2004).

<sup>15</sup>R. H. T. Wilke *et al.*, Phys. Rev. Lett. **92**, 217003 (2004).

<sup>16</sup>E. Ohmichi *et al.*, J. Phys. Soc. Jpn. **73**, 2065 (2004).

<sup>17</sup>P. P. Singh, Solid State Commun. **127**, 271 (2003).

<sup>18</sup>J. Kortus *et al.*, Phys. Rev. Lett. **94**, 027002 (2005)

<sup>19</sup>G. A. Ummarino *et al.*, cond-mat/0408702, Phys. Rev. B (to be published).

<sup>20</sup>S. C. Erwin and I. I. Mazin, Phys. Rev. B **68**, 132505 (2003).

<sup>21</sup>Similar results were obtained for  $\mathbf{B} \parallel ab$ , as we will discuss in a forthcoming paper.